

## Large Conductance Modulation of Gold Thin Films by Huge Charge Injection via Electrochemical Gating

D. Daghero,\* F. Paolucci,<sup>†</sup> A. Sola,\* M. Tortello,\* G. A. Ummarino,\* M. Agosto, and R. S. Gonnelli\*

*Dipartimento di Fisica, Politecnico di Torino, 10129 Torino, Italy*

Jijeesh R. Nair\* and C. Gerbaldi\*

*Dipartimento di Scienza dei Materiali e Ingegneria Chimica, Politecnico di Torino, 10129 Torino, Italy*  
(Received 15 August 2011; revised manuscript received 20 December 2011; published 10 February 2012)

By using an electrochemical gating technique with a new combination of polymer and electrolyte, we were able to inject surface charge densities  $n_{2D}$  as high as  $3.5 \times 10^{15} e/\text{cm}^2$  in gold films and to observe large relative variations in the film resistance,  $\Delta R/R'$ , up to 10% at low temperature.  $\Delta R/R'$  is a linear function of  $n_{2D}$ —as expected within a free-electron model—if the film is thick enough ( $\geq 25$  nm); otherwise, a tendency to saturation due to size effects is observed. The application of this technique to 2D materials might allow extending the field-effect experiments to a range of charge doping where large conductance modulations and, in some cases, even the occurrence of superconductivity are expected.

DOI: 10.1103/PhysRevLett.108.066807

PACS numbers: 73.20.-r, 73.61.At, 82.47.Uv

Since the 1960s, the possibility to modulate the transport properties of various materials by means of the so-called field effect (FE) has attracted much interest. Apart from the nowadays obvious application in semiconductor-based electronic devices such as field-effect transistors (FETs), the technique has been widely used also for more exotic purposes. It has allowed enhancing the critical temperature of some superconductors [1–3], inducing metallic behavior in insulators [4] or even a superconducting phase transition in materials like SrTiO<sub>3</sub> [5], ZrNCl [6], and KTaO<sub>3</sub> [7]. In the standard FET configuration, the maximum density of the induced surface charge,  $\sigma_{\text{max}}$ , is of the order of  $10^{13}$  charges  $\text{cm}^{-2}$  if suitable dielectrics are used. Only with a polymeric gating technique [8,9], electric fields as high as 100 MV/cm and surface carrier concentrations of  $10^{14}/\text{cm}^{-2}$  [6] have been achieved. The present record, to the best of our knowledge, is  $4.5 \times 10^{14} \text{ cm}^{-2}$  [10]. The reason of this order-of-magnitude improvement with respect to the conventional FETs is the formation of the electric double layer (EDL) at the interface between the electrolyte solution and the sample surface. The EDL acts as a parallel-plate capacitor with an extremely small distance between the plates (of the order of the polymer molecule size) [6] and thus a very large capacitance.

Here, we will show that a new polymeric electrolyte solution (PES) allows further extending the surface charge density to some units in  $10^{15}$  charges  $\text{cm}^{-2}$  for applied voltages of the order of a few volts (5 V at most), which marks a significant improvement with respect to the present state of the art. In particular, we will apply this technique to Au films.

The FE in metals has been devoted little attention, either because of its little practical interest or because it is often believed to be unobservable. Indeed, in the semi-classical, metallic limit, the electronic screening length

(the Thomas-Fermi radius) is less than one atomic diameter. Nonetheless, a modulation of the conductivity of metal films (including Au) has been obtained already in the 1960s [11,12] with a conventional gating technique. These and the following measurements of the same kind [1,13–15] have evidenced a number of unexpected properties and differences between metals that well justify a fundamental interest in this topic—especially because most of these results have not found a really exhaustive explanation up to now.

We will leave the fundamental study of the FE in gold and other metals (Cu, Ag) to a following paper. Here, we will just focus on the technique that allows extending the field-effect studies to unprecedented surface charge densities. In particular, we will show that this technique allows observing very large modulations in the gold resistivity both at room temperature and at cryogenic temperatures. The relative variation of the film resistance  $\Delta R/R'$  produced by the transverse electric field can be as high as 10% at low temperature and perfectly extends the analogous results obtained at much smaller charge densities by using the standard FET configuration.

The field-effect devices (FEDs) were fabricated on glass, SiO<sub>2</sub>, or Si<sub>3</sub>N<sub>4</sub> substrates and were designed in a completely planar configuration, as in Ref. [9], with the film under study and all the electrodes (drain, source, contacts for voltage measurement, and gate) on the same plane. A picture of a device on SiO<sub>2</sub> is shown in Fig. 1(a).

The gold films were deposited by physical vapor deposition (PVD) at a pressure  $P \sim 2 \times 10^{-5}$  mbar, in the forms of a thin strip. The thickness of the films, measured by means of a profilometer and/or an atomic force microscope, ranges between 10 and 50 nm. Scanning electron microscopy (SEM) images of the film surface [Fig. 1(b)] show accretion islands connected to form a continuous

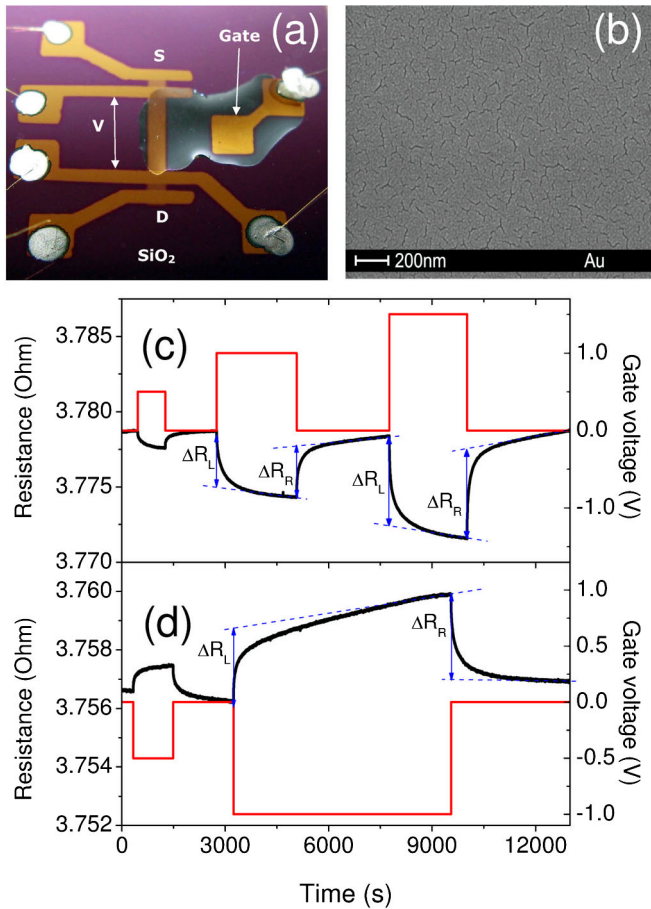


FIG. 1 (color online). (a) Photograph of a Au FED on a  $\text{SiO}_2$  substrate.  $D$  and  $S$  are the drain and source contacts; the voltage is measured between the inner contacts. The drop of polymer electrolyte covers the part of the film between the voltage contacts as well as the gate electrode. (b) SEM image of the Au film. (c),(d) Typical response of the film resistance to positive and negative gate voltages.

network. This kind of structure is typical of the best gold films grown by PVD, as reported in the literature [16]. The four gold electrodes for current feeding and voltage measurement, as well as the gate electrode, were then deposited on top of the film by PVD at  $P \sim 4 \times 10^{-5}$  mbar and are much thicker than the film. The polymer electrolyte solution we used was obtained by a reactive mixture of bisphenol A ethoxylate (15 EO/phenol) dimethacrylate (BEMA; average  $M_n$ : 1700, Aldrich), poly(ethylene glycol)methyl ether methacrylate (PEGMA; average  $M_n$ : 475, Aldrich), and lithium bis(trifluoromethanesulfonyl)imide (LiTFSI) in the presence of 3% wt of a 2-hydroxy-2-methyl-1-phenyl-1-propanone free radical photoinitiator (Darocur1173, Ciba Specialty Chemicals). For detailed characteristics of the polymer electrolyte and related components, see Ref. [17] and references therein. The quantities of BEMA and PEGMA are in a 3:7 ratio, and the LiTFSI is the 10% wt of the total compound.

The PES was put on top of the device, so as to cover the whole portion of the film between the voltage electrodes as well as the gate electrode, as shown in Fig. 1(a). Since the area of the gate electrode is larger than that of the film, there is no need for reference electrodes [18]. The PES was then polymerized by UV exposure using a medium vapor pressure Hg UV lamp (Helios Ital quartz, Italy), with a radiation intensity on the surface of the sample of  $30 \text{ mW cm}^{-2}$ . All the above operations were performed in a controlled Ar atmosphere of a dry glove box (MBraun Labstar,  $\text{O}_2$  and  $\text{H}_2\text{O}$  content  $< 0.1$  ppm).

The field-effect devices were then mounted in a pulse-tube cryocooler and kept in a high vacuum to protect the PES from moisture and chemical contaminations. Figures 1(c) and 1(d) show the effect of positive and negative voltage steps (applied at  $T_{\text{room}} = 295$  K, above the glassy transition of the polymer that occurs at about 210 K) on the resistance of the film, measured with the four-terminal technique with a dc current of 1–5 mA. To eliminate the possible contributions of thermoelectric effects and of the dc gate current to the measured resistance, the current was inverted in each measurement; i.e., the resistance was calculated as  $R = (V_+ - V_-)/(2I)$ ,  $V_{\pm}$  being the voltage for forward (backward) current. We have experimentally demonstrated that this technique gives the same results as a low-frequency (133.33 Hz) lock-in technique. The film resistance is related to the applied voltage through the charge on the EDL. For a given gate voltage  $V_G$ , the resistance variation  $\Delta R = [R(V_G) - R_0]$  [where  $R_0 = R(V_G = 0)$ ] is obtained by averaging the resistance jumps  $\Delta R_L$  and  $\Delta R_R$  on applying and removing the gate voltage, as shown in Fig. 1.

The problem then arises of how to relate the gate voltage to the charge of the EDL and thus to the density of the surface charge injected in the film. Hall-effect measurements would require huge magnetic fields because of the high intrinsic carrier density of Au. Moreover, determining the charge of the EDL by integrating the gate current is not correct if electrochemical effects are present, as pointed out in Ref. [18]. Electrochemical impedance spectroscopy measurements carried out both on our devices and on a steel/PES/steel cell showed indeed that electrochemical effects take place at frequencies below 10 Hz [18]. We thus used a procedure called *double-step chronocoulometry* [19] that allows separating the electrostatic charge we are interested in from the charge that flows through the PES because of electrochemical effects (e.g., diffusion of electroreactants).

Figure 2 shows the time dependence (a) of the gate current  $I_G$  and (b) of the total charge  $Q(t) = \int_0^t I_G(t') dt'$  when a gate voltage of 1 V is applied and then removed. The curves are very similar to the typical ones depicted in [19]. Note that, after the first voltage step, a nonvanishing gate current continues to flow indefinitely. This current is always various orders of magnitude smaller than the probe

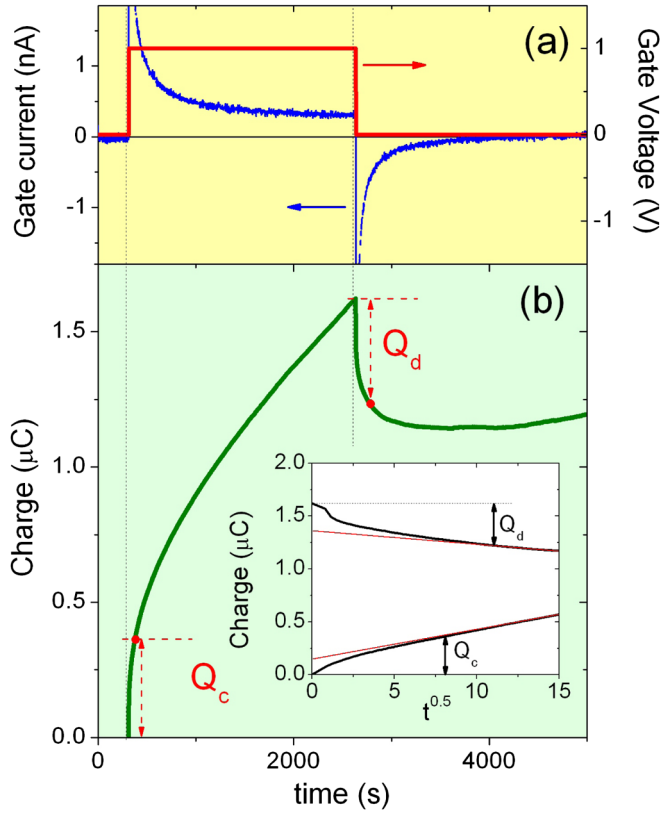


FIG. 2 (color online). Time dependence of (a) the gate voltage and current, and (b) the charge obtained by integration of the current, when a gate potential of +1 V is applied and removed. The dots on the curves in (b) indicate the points where the EDL is completely charged or discharged. The length of the dashed arrows corresponds to the injected charge  $Q_c$  and  $Q_d$ , obtained by means of a chronocoulometric procedure. As shown in the inset,  $Q_c = Q(t^*)$ , where  $t^*$  is the time at which the  $Q(t)$  curve starts to be linear as a function of  $t^{1/2}$ .  $Q_d$  is determined in a similar way.

current in the film (1–5 mA) [20] and is due to the flow of charges necessary to maintain the gradient of ion concentration when tunneling effects through the EDL [18] or diffusion of electroreactants [19] take place. The shape of  $Q(t)$  shows indeed that two phenomena occur on very different length scales: a rather fast EDL charging or discharging (that gives  $Q$  an exponential time dependence) and other effects of electrochemical nature that give a  $t^{1/2}$  dependence. In analogy with the chronocoulometry method, we determined the time  $t^*$  at which  $Q(t)$  starts to become linear as a function of  $\sqrt{t}$ , as shown in the inset to Fig. 2(b), and assumed that the total charge “injected” in the film surface is  $Q(t^*)$ . Clearly, two values are obtained,  $Q_c$  and  $Q_d$ , for the charge and discharge phases. Normally, they coincide within the experimental uncertainty; this indicates that no adsorption of reactants or products occurs [19]. The injected charge is finally defined as  $Q_i = (Q_c + Q_d)/2$ . In the few cases where  $Q(t)$  deviates from the aforementioned behavior in one of the two

steps (charge or discharge),  $Q_i$  is determined by the other step.

Once  $Q_i$  is known, we define the surface density of injected carriers as  $n_{2D} = Q_i/eS$ , where  $S$  is the surface of the film covered by the polymer (gated area) and  $e$  is the electronic charge. Obviously, the charge distribution on the surface is not exactly 2D but, if  $z$  is the axis normal to the interface, it follows a density profile  $n_{3D}(z)$  which decays on a length scale defined by the screening length  $\xi$ . Thus,  $n_{2D}$  is the integral of  $n_{3D}(z)$  over the whole thickness of the perturbed layer. Clearly,  $n_{3D}(z)$  and  $\xi$  depend on the material under study, e.g., on whether it is a metal or a semiconductor. In the case of our Au films and within a simplified semiclassical model, one can imagine that the whole injected charge is uniformly distributed in a surface layer of thickness  $\approx \xi$  so that  $n_{3D} = n_{2D}/\xi$  and that the film behaves as the parallel of the perturbed and unperturbed regions. A trivial free-electron calculation (assuming constant effective electron mass and relaxation time) of the resistance of the whole film gives

$$\Delta R/R' = \frac{R(V_G) - R_0}{R(V_G)} = -\frac{n_{2D}}{nt}, \quad (1)$$

where  $n$  is the unperturbed 3D density of charge carriers. In this equation,  $\Delta R/R'$  does not depend explicitly on  $\xi$  but only on the whole film thickness  $t$  and, of course, on  $n_{2D}$ . A more sophisticated perturbative self-consistent quantum approach based on the Lindhard-Hartree theory of the electronic screening [21], including a proper model of the film conduction (e.g., accounting for the probability  $p$  of electronic specular reflection at the film surface [22]), gives a similar equation, but with an additional factor that depends in a complicated way on  $t$  and  $p$ . This term reduces to 1 when  $p = 0$ . Further details will be given elsewhere [21].

Figure 3 shows that, for the great majority of the devices studied here,  $t\Delta R/R'$  is a linear function of  $n_{2D}$ , in agreement with Eq. (1) [23]. Vertical and horizontal error bars account for the difference in the values of  $\Delta R/R'$  and  $n_{2D}$  determined in the charging and discharging phases—i.e., on application and removal of the gate voltage, see Figs. 1(c) and 1(d) and the inset to Fig. 2(b). Note that the small rectangular region around the origin of the axes of Fig. 3 includes the values of  $n_{2D}$  reported so far in the literature. A magnification of this region is shown in the upper inset. The values of  $n_{2D}$  obtained with our technique extend instead up to  $3.5 \times 10^{15}$  electrons/cm<sup>2</sup>. The same linear trend is common to all devices, but some deviations occur in the thinner ones at higher charge densities. This is not surprising, since, in these films, the surface scattering plays a major role, and the simple free-electron model [Eq. (1)] breaks down. A reduction in the absolute value of  $\Delta R/R'$  for a given  $n_{2D}$  is indeed predicted by the aforementioned quantum perturbative model [21] when

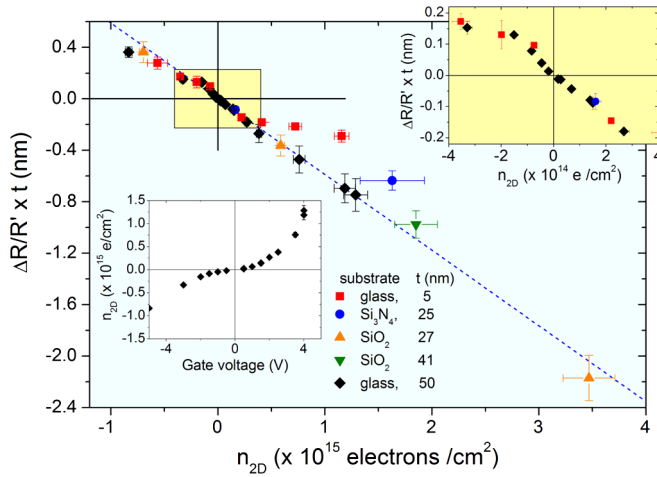


FIG. 3 (color online). Dependence of  $\Delta R/R't$  on  $n_{2D}$  (i.e., number of electrons per  $\text{cm}^2$ ) as obtained for various films with different thickness and on different substrates, indicated in the legend. The straight dotted line is a guide for the eyes. The upper inset shows a zoom around the origin of the axes. The lower inset shows the dependence of  $n_{2D}$  on the gate voltage, for the 50-nm-thick Au film.

the probability of electron reflection at the surface [22] is not negligible.

In view of the application of this gating technique to more interesting 2D materials, like graphene and multi-layer graphene, graphane [25],  $\text{MoS}_2$ , BN,  $\text{NbSe}_2$ , and so on—in particular, to see whether some of these materials can develop superconductivity upon charge doping—it is important to check what happens when the device is cooled

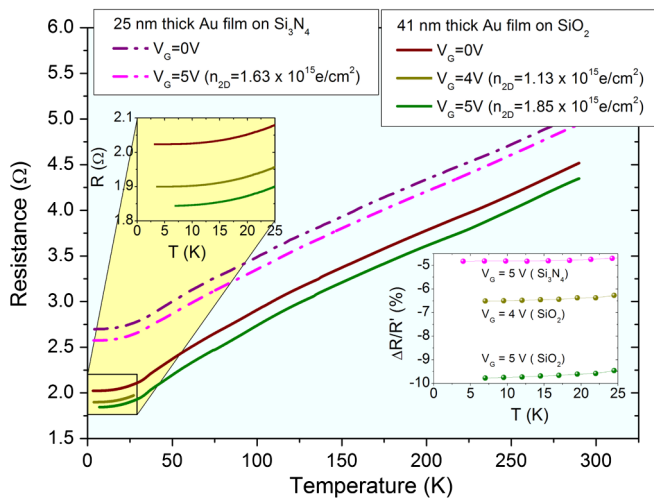


FIG. 4 (color online). Temperature dependence of the resistance of two Au films for different values of the gate voltage. The corresponding values of  $n_{2D}$ , measured at room temperature, are indicated in the legend. Upper inset: zoom of the low-temperature region. Lower inset: relative resistance variation  $\Delta R/R'$  at low temperatures, extracted from the curves in the main panel.

to cryogenic temperatures. Because of the glassy transition of the polymer at  $T_{\text{glass}} \approx 210$  K and the consequent “freezing” of the EDL charge below that threshold, the gate voltage must be applied at  $T > T_{\text{glass}}$  and kept constant on cooling. As expected, the gate current that persists after the EDL charge [see Fig. 2(a)] and that is related to the ionic flow in the polymer electrolyte goes smoothly to zero on crossing the glassy transition, but this does not affect the film resistance. Incidentally, this further confirms that the observed resistance modulation is not an artifact due to the gate current. The cooling speed should be small enough to avoid cracks in the film or in the contacts due to the abrupt thermal contraction of the polymer. The  $R(T)$  curve is then measured on slowly heating the FED from the lowest temperature (here about 3.3 K) to room temperature. Figure 4 shows the  $R(T)$  curves for two Au films on different substrates, i.e.,  $\text{Si}_3\text{N}_4$  (dot-dashed lines) and  $\text{SiO}_2$  (solid lines). The curves at  $V_G = 0$  and  $V_G = 5$  V are shown for both devices; for the latter, an additional curve at  $V_G = 4$  V is reported, although it extends only up to 28 K because one of the contacts broke down at that temperature. A large offset is observed within each series, due to the applied field. The lower inset shows the low-temperature values of  $\Delta R/R'$  extracted from these curves. At the lowest temperatures, the resistance varies by almost 10%, which is a huge quantity for a noble metal. Incidentally, preliminary measurements on Cu films indicate an even larger effect (up to 30%).

Finally, Fig. 5 reports and compares in log-log scale some results obtained in Au devices of different kinds, i.e., based on PESs with different compositions, and also in conventional back-gate field-effect devices made by depositing the Au film and the electrodes on top of a suspended SiN membrane [26] with the Au gate electrode

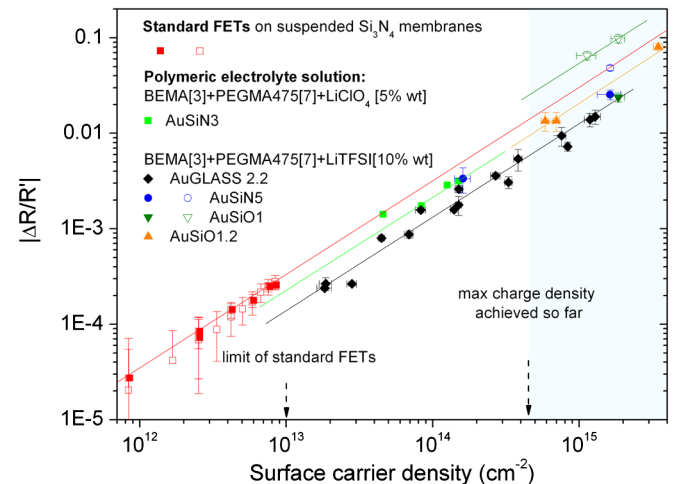


FIG. 5 (color online). Logarithmic plot of  $|\Delta R/R'|$  vs the surface density of charge carriers in standard back-gate FETs and in devices made with two different kinds of PES. Solid (open) symbols indicate data taken at room temperature (low temperature).

on the other side. The figure clearly shows that  $|\Delta R/R'|$  is a linear function of  $|n_{2D}|$  for all kinds of devices; the vertical offset of the parallel trend lines is mainly due to the different thicknesses of the films.

In conclusion, we have shown that, with a suitable polymeric electrolyte solution, it is possible to extend the range of surface charge densities achieved in field-effect experiments (even at cryogenic temperatures) to a maximum of some units in  $10^{15}$  charges/cm<sup>2</sup>. These values are well in the range where large modulations of the conduction properties of some 2D materials and even the occurrence of superconductivity (e.g., in graphane [25]) have been predicted. For the time being, we have shown that these carrier injections give rise to variations in the resistance of Au thin films up to about 10%. The quantity  $\Delta R/R'$  for a given device linearly depends on  $n_{2D}$ , while *all* the data follow a universal linear trend if a proper normalization to the film thickness is used. Some deviations are observed in very thin films, where the free-electron model is unable to describe the conduction. These deviations are however compatible with more sophisticated perturbative quantum models.

---

\*Present address: Dipartimento di Scienza Applicata e Tecnologia, Politecnico di Torino, 10129 Torino, Italy.

†Present address: Max Planck Institute for Solid State Research, D-70569 Stuttgart, Germany.

- [1] R. E. Glover, III and M. D. Sherrill, *Phys. Rev. Lett.* **5**, 248 (1960).
- [2] J. Mannhart *et al.*, *Z. Phys. B* **83**, 307 (1991).
- [3] C. H. Ahn *et al.*, *Science* **284**, 1152 (1999).
- [4] H. Shimotani *et al.*, *Appl. Phys. Lett.* **91**, 082106 (2007).
- [5] K. Ueno *et al.*, *Nature Mater.* **7**, 855 (2008).
- [6] J. T. Ye *et al.*, *Nature Mater.* **9**, 125 (2010).
- [7] K. Ueno *et al.*, *Nature Nanotech.* **6**, 408 (2011).
- [8] M. J. Panzer, C. R. Newman, and C. D. Frisbie, *Appl. Phys. Lett.* **86**, 103503 (2005).
- [9] A. S. Dhoot *et al.*, *Proc. Natl. Acad. Sci. U.S.A.* **103**, 11 834 (2006).
- [10] H. T. Yuan *et al.*, *Adv. Funct. Mater.* **19**, 1046 (2009).
- [11] G. Bonfiglioli and R. Malvano, *Phys. Rev.* **115**, 330 (1959).
- [12] G. Bonfiglioli and R. Malvano, *Phys. Rev.* **101**, 1281 (1956).
- [13] H. L. Stadler, *Phys. Rev. Lett.* **14**, 979 (1965).
- [14] G. Martinez-Arizala *et al.*, *Phys. Rev. Lett.* **78**, 1130 (1997).
- [15] N. Marković *et al.*, *Phys. Rev. B* **65**, 012501 (2001).
- [16] L. Zhang *et al.*, *Surf. Sci.* **439**, 73 (1999).
- [17] J. R. Nair, C. Gerbaldi, M. Destro, R. Bongiovanni, and N. Penazzi, *React. Funct. Polym.* **71**, 409 (2011).
- [18] H. Yuan *et al.*, *J. Am. Chem. Soc.* **132**, 18 402 (2010).
- [19] G. Inzelt, in *Electroanalytical Methods: Guide to Experiments and Applications*, edited by F. Scholz (Springer-Verlag, Berlin, 2010), p. 147.
- [20] For example, when a gate voltage  $V_G = 1$  V was applied,  $I_G$  saturated at 1 nA or even less [see Fig. 2(a)]. The maximum value of the residual gate current (measured when  $V_G = 5$  V) was 600 nA, which is only 0.06% of the probe current.
- [21] M. Omini *et al.* (unpublished).
- [22] K. Fuchs, *Proc. Cambridge Philos. Soc.* **34**, 100 (1938).
- [23] The thickness of the thinner film (5 nm) results from a correction that accounts for the voids in polycrystalline films that reduce the actual film cross section (see Ref. [24]). In the other cases, the correction was not necessary.
- [24] J. M. Rowell, *Supercond. Sci. Technol.* **16**, R17 (2003).
- [25] G. Savini, A. C. Ferrari, and F. Giustino, *Phys. Rev. Lett.* **105**, 037002 (2010).
- [26] D. Delaude, Ph.D. thesis, Politecnico di Torino, 2009 (unpublished).